Mon. Not. R. astr. Soc. (1983) **204**, 791–810

Kinematical and chemical evolution of the galactic disc

Cedric G. Lacey *Institute of Astronomy, Madingley Road, Cambridge CB3 0HA and Department of Astrophysical Sciences, Princeton, New Jersey, USA*

S. Michael Fall *Institute of Astronomy, Cambridge and Institute for Advanced Study, Princeton, New Jersey, USA*

Received 1982 November 16; in original form 1982 July 28

Summary. In the models presented here, metal-free gas accumulates in the galactic disc at a rate that decays exponentially on a time-scale t_f. Stars then form with a constant initial mass function and a small velocity dispersion at a rate proportional to the nth power of the volume density of the gas layer. They are stochastically accelerated in such a way that the q th power of their velocity dispersion in the vertical direction increases at a rate proportional to the rate of star formation. Chemical enrichment is treated in the approximation of instantaneous recycling with no exchange of material between different galactocentric radii. The models are first compared with the observed dependence of metallicity and velocity dispersion on age and the distribution of metallicities for stars in the solar neighbourhood. These relations are satisfied by models with $n = 1$ and $t_f = 5.5$ Gy or $n = 3/2$ and $t_f = 3.5$ Gy and $1.5 \lesssim q \lesssim 2.5$. This range of q brackets the values needed to explain the nearly constant scale-heights observed in the stellar discs of edge-on galaxies. The models that are successful in the solar neighbourhood also reproduce the observed variation of gas density and star formation rate between galactocentric radii of 4 and 14 kpc but they do not reproduce the observed gradient in metallicity.

1 Introduction

A natural and now standard explanation for the structure of our Galaxy is that the bulge component formed first in a relatively rapid collapse and the disc component formed later in a relatively slow collapse. Two alternatives have been considered for the subsequent evolution of the disc, as reflected in the kinematical properties of stars in the solar neighbourhood. In one view, the correlation between velocity dispersion and age is explained by the birth of stars in a slowly settling layer of gas (Blaauw 1965 and references therein). In the other view, which originated with Spitzer & Schwarzschild (1951, 1953), this correlation is explained by the stochastic acceleration of stars after their birth in a thin layer of gas.

From a careful study of the observational data, Wielen (1977) concludes that they are explained most naturally by the acceleration mechanism.

Much of the discussion of chemical evolution in the solar neighbourhood has centred on the so-called G dwarf problem, which was first recognized by van den Bergh (1962) and Schmidt (1963). Simple closed models – those that start with metal-free gas, have no inflows or outflows and form stars with a constant initial mass function – produce more metal-poor stars than are observed. Larson (1972) suggested that the infall of primordial gas might resolve this discrepancy and his hydrodynamical calculations later showed that a prolonged period of infall might be a natural consequence of galaxy formation (Larson 1976). Among several possible solutions of the G dwarf problem, this is perhaps the most attractive one from a theoretical point of view but there is little direct observational evidence for it. Much of the recent work on the chemical evolution of galaxies has been reviewed by Tinsley (1980) and Pagel (1981).

Our purpose in this paper is to present a series of models for the kinematical and chemical evolution of the galactic disc. The primary motivation for this project was an attempt to reconcile the observational data on the rate of star formation and stochastic acceleration in the solar neighbourhood with the photometry of edge-on discs by van der Kruit & Searle (1981a, b). Although our models differ in several respects from previous models, they are natural extensions of contemporary work in this field. For example, Chiosi (1980) studied the effects of infall on metallicity gradients in the galactic disc and Vader & de Jong (1981) studied the connection between stochastic acceleration and chemical evolution in the solar neighbourhood. The novel feature of the present investigation is that we combine all these ingredients and make a detailed comparison with the observations.

2 Basic assumptions and equations

2.1 THE INFALL OF GAS

The rate of change of mass at any galactocentric radius is assumed to be governed solely by the infall of gas from outside the disc. This implies

$$\frac{\partial}{\partial t}(\mu_s + \mu_g) = f \tag{1}$$

where μ_s and μ_g are respectively the surface densities of stars and gas and f is the infall rate per unit area. The category 'stars' includes inert remnants as well as nuclear-burning objects and the category 'gas' includes both the atomic and molecular components of the interstellar medium. To insure that the density profile of the disc is always exponential with a scale-radius α^{-1}, we adopt an infall rate of the form

$$f(r, t) = \mu_0 \exp(-\alpha r) F(t). \tag{2}$$

Here μ_0 is the central density at the present epoch, which we denote $t = T_1$, and $F(t)$ is normalized so that its integral from $t = 0$ to T_1 is unity.

In most of the models, the infall rate is assumed to decay exponentially with a time-scale t_f; thus

$$F(t) = \frac{\exp(-t/t_f)}{t_f[1 - \exp(-T_1/t_f)]}. \tag{3}$$

In the absence of a comprehensive theory for the infall process, this expression is intended as a simple one-parameter model with reasonable characteristics. The higher rate at early times

may be associated with the collapse of material during the formation of the Galaxy and the lower rate at late times may be associated with the accretion of intergalactic material. In a few of the models the functional form of $F(t)$ is modified as a described in Section 4.2 or the time-scale t_f is allowed to vary with radius as described in Section 4.4. The consequences of neglecting radial flows in the disc are discussed in Section 4.5.

2.2 THE FORMATION OF STARS

Stars are assumed to form with a constant initial mass function (IMF) at a rate per unit area ψ, that varies with the properties of the gas. In the approximation of instantaneous recycling, the surface density of stars is governed by the equation

$$\partial \mu_s / \partial t = (1-R)\psi \tag{4}$$

where the returned fraction, R, is a constant. The value of this parameter is uncertain as a result of uncertainties in the IMF and the masses of stellar remnants but it probably lies in the range $0.1 \lesssim R \lesssim 0.5$ (Tinsley 1981). The conditions for the validity of equation (4) are less restrictive than those for chemical evolution in the approximation of instantaneous recycling, which is discussed in Section 2.5.

Following Schmidt (1959), we assume that the star formation rate per unit volume is proportional to ρ_g^n where ρ_g is the volume density of the gas and the parameter n depends on the specific mechanism involved. For example, $n \approx 3/2$ is appropriate if stars form on the free-fall time-scale of individual clouds and $n \approx 2$ is appropriate if they form on the time-scale for collisions between clouds (Larson 1977). An integration through the disc (z-direction) gives

$$(1-R)\psi = CH_g(\mu_g/H_g)^n \tag{5}$$

where H_g is a measure of the vertical extent of the gas layer, which we take to be its half-thickness, $\mu_g/2\rho_g(z=0)$. The coefficient in this expression has been defined so that a specific value of R is not needed in our model computations. To the extent that $\rho_g(z)$ evolves homologously, with simple scalings in μ_g and H_g, C is a constant that depends on R and n. The effects of varying C with galactocentric radius are explored in Section 4.4 but otherwise C and n are held fixed in each of the models.

In a few of the models, star formation is prevented until enough gas accumulates to satisfy the criterion for gravitational instability derived by Goldreich & Lynden-Bell (1965). For a disc with a flat rotation curve of amplitude v_m, this is

$$G\mu_g \gtrsim 0.47\,\sigma_g(\sqrt{2}v_m/r) \tag{6}$$

where σ_g is the velocity dispersion of the gas in any one dimension and the quantity in brackets is the epicyclic frequency at the radius r. In this case, no stars form until the time $t_*(r)$ when equation (6) is first satisfied and afterwards they form at the rate given by equation (5), irrespective of whether equation (6) is satisified. The motivation for this procedure is that star formation may be inhibited in regions that are stabilized against large-scale clumping (Fall & Efstathiou 1980).

2.3 THE STOCHASTIC ACCELERATION OF STARS

Stars are assumed to form with a velocity dispersion σ_{s0} that is comparable with the velocity dispersion in the gas. They are then accelerated by the irregular gravitational field of 'clumps' in the disc, which results in the diffusion of their orbits. Following Wielen (1977),

we assume that the velocity dispersion in the vertical direction of stars of the same age is governed by the equation

$$\partial \sigma_s^2/\partial t \propto \mu_c \sigma_s^{2-q}. \tag{7}$$

Here μ_c is the surface density of clumps and the right-hand side of the equation represents a 'diffusion coefficient' with an exponent q to be determined. Any dependence of the acceleration rate on the amplitudes of the vertical motions of the stars is assumed to be through σ_s and is therefore reflected in the value for q. For comparison with theoretical calculations, we note that the asymptotic solution of equation (7) is $\sigma_s \sim t^{1/q}$ when μ_c is constant.

Most theoretical calculations of the diffusion process have been restricted to horizontal motions in the disc. Spitzer & Schwarzschild (1953) considered acceleration by long-lived clouds and found precisely equation (7) with $q = 3$. If the lifetimes of the clouds are shorter than the time-scale for interactions between the stars and clouds, the diffusion coefficient should be independent of velocity (Fujimoto 1980). As Julian (1967) has shown, the gravitational response of the stars to the clouds will act as a further source of perturbation to their velocities with $2 \lesssim q \lesssim 3$. In the extreme form of this mechanism, the stars react to a series of transient density waves in the disc, which leads to $q = 2$ if the fluctuations occur on time-scales shorter than the period of galactic rotation (Barbanis & Woltjer 1967). A theoretical analysis of stochastic acceleration in the vertical direction, with allowance for the finite thickness of the layers of stars and clumps will be given in a separate investigation (Lacey, in preparation). Preliminary results indicate that the exponent is larger in this case but that it is not far from the range $2 \lesssim q \lesssim 3$ for purely horizontal motions.

To connect the diffusion rate with the star formation rate, we assume proportionality between ψ and μ_c. In this case, equations (4) and (7) give

$$\partial \sigma_s^q/\partial t = \beta \partial \mu_s/\partial t \tag{8}$$

where β is a parameter that depends only on the intrinsic properties of the clumps, such as their masses and sizes, but not on their mean density. This assumption is especially reasonable if the clumps are identified with molecular clouds because they appear to be the major sites of star formation. It may also be reasonable if the clumps are identified with irregularities on larger scales, such as spiral density waves, because they also show strong correlations with star formation. In addition to this stochastic acceleration, the velocities of stars will change in reaction to the increasing gravitational field caused by the infall of material on to the disc. As shown in Section 4.5, this effect is negligible after a few times 10^8 yr and we therefore ignore it in the models.

We can now integrate equation (8) to derive the velocity dispersion at time t of stars born at time t_0:

$$\sigma_s^q(t; t_0) = \sigma_{s0}^q + \beta[\mu_s(t) - \mu_s(t_0)]. \tag{9}$$

Then the mean square velocity of all stars born up to the time t in the disc is

$$\begin{aligned}\sigma_{sm}^2(t) &= \frac{1}{\mu_s(t)} \int_0^t dt_0 \, \sigma_s^2(t; t_0) \, d\mu_s(t_0)/dt_0 \\ &= \frac{1}{\mu_s(t)} \int_0^{\mu_s(t)} dx \left\{\sigma_{s0}^q + \beta[\mu_s(t) - x]\right\}^{2/q} \\ &= \frac{q[\sigma_{s0}^q + \beta\mu_s(t)]^{2/q+1} - q\sigma_{s0}^{q+2}}{\beta(2+q)\mu_s(t)}\end{aligned} \tag{10}$$

where σ_{s0} is assumed to be constant. We emphasize that the validity of equation (8) and the consequent equations (9) and (10) is not affected by the other details of the models presented here.

2.4 VERTICAL EXTENT OF THE GAS AND STARS

The galactic disc is assumed to be self-gravitating in the vertical direction and the layers of gas and stars are assumed to be in hydrostatic equilibrium at all times. To relate the half-thicknesses of these components with their surface densities and velocity dispersions, we use the approximations derived by Talbot & Arnett (1975) for locally isothermal sheets:

$$\sigma_g/H_g \approx \sigma_{sm}/H_s \approx \pi G(\mu_g/\sigma_g + \mu_s/\sigma_{sm}). \tag{11}$$

Here, σ_{sm} is assumed to be given by equation (10) and σ_g is assumed to be a suitable average over all the motions in the gas when this is idealized as a single component. Talbot & Arnett (1975) argue that σ_g is maintained at a roughly constant value by a stable feedback mechanism that balances the energy injected by supernovae with the energy dissipated by cloud collisions. This is reasonable if the properties of the clouds have remained similar over the life-time of the disc as is assumed in our models.

In some applications, the exponential scale-height of the stellar disc is a more useful measure of its vertical extent than is the half-thickness. At large $|z|$, the gravitational field is approximately $\pm 2\pi G(\mu_s + \mu_g)$ and the density profile of a locally isothermal sheet declines as $\exp(-|z|/h_s)$ with a scale-height given by

$$h_s = \sigma_{sm}^2/2\pi G(\mu_s + \mu_g). \tag{12}$$

This result can be combined with equation (10) to derive an expression that is valid for any ratio of star-to-gas densities. In the limits $\mu_s \gg \mu_g$ and $\beta\mu_s \gg \sigma_{s0}^q$, we find

$$h_s \approx \left(\frac{q}{q+2}\right)\frac{\beta^{2/q}}{2\pi G}\,\mu_s^{2/q-1}. \tag{13}$$

For the particular case that the diffusion parameters are $q = 2$ and $\beta =$ constant the scale-height of the stars is independent of μ_s and therefore independent of galactocentric radius.

2.5 CHEMICAL EVOLUTION OF THE DISC

The heavy elements in the disc are assumed to be enriched by stellar ejecta and diluted by infalling material. In the approximation of instantaneous recycling, the abundance of primary elements in the gas, Z_g, is governed by the equation

$$\mu_g \partial Z_g/\partial t = y(1-R)\psi - fZ_g \tag{14}$$

where the bulk yield, y, is a constant. A term fZ_f must be added to the right-hand side of this expression if the infalling gas has a metallicity Z_f but this is assumed to be negligible in our models. Talbot & Arnett (1971) have shown that the approximation of instantaneous recycling is accurate to within about 10 per cent when the gas fraction exceeds 0.1 in closed models. When this condition is violated, the predicted values of Z_g are too high at given values of μ_g/μ_s. A less restrictive condition applies to infall models so equation (14) should be adequate for most of the galactic disc over most of its life-time.

The bulk yields computed by Arnett (1978) and Maeder (1981) from evolutionary models of massive stars are $y \approx 0.012$. Apart from uncertainties in the stellar structure and

nucleosynthesis, these estimates could be off by factors of 3 or more as a result of uncertainties in the relative normalization of the initial mass function above and below the present turnoff. A more reliable prediction is the present ejection rate of new metals, for which Maeder computes $y(1-R)\psi_1 \approx 0.04\, M_\odot\, \mathrm{pc}^{-2}\, \mathrm{Gy}^{-1}$ with the high-mass end of the Miller–Scalo (1979) IMF. Since the yield enters equation (14) through the combination Z_g/y, we determine y by scaling to match the observations of Z_g. In the applications to stellar data, we omit the subscript g with the understanding that $Z(t)$ is the metallicity of stars that formed at time t.

2.6 INTEGRATION OF THE EQUATIONS

Our models are defined by equations (1) to (6), equations (10) to (12) and equation (14). In addition, we impose the boundary conditions that μ_s, μ_g and Z_g vanish at time $t = 0$ for all galactocentric radii r. Since none of the derivatives involves r, this system reduces to a set of ordinary differential equations with t as the independent variable. In the special case that $n = 1$, they can all be integrated analytically and this provides a useful check on the numerical integrations. As inputs, we require the disc parameters μ_0, α^{-1} and v_m and the velocity dispersion of the gas σ_g. These are taken from observation and are fixed throughout. As outputs, we obtain $\mu_s(r,t)$, $\mu_g(r,t)$, $Z_g(r,t)/y$, $\sigma_s(r,t)$, $(1-R)\psi(r,t)$ and related functions. The infall time-scale t_f, the star formation parameters C and n, the diffusion parameters β and q and the initial velocity dispersion of the stars σ_{s0} are then adjusted to fit the corresponding observations.

3 Observational parameters and relations

3.1 CHEMICAL EVOLUTION IN THE SOLAR NEIGHBOURHOOD

As the primary guide to chemical enrichment, we use the relation between metallicity and age derived by Twarog (1980) and shown in Fig. 1. This is based on fits of the Yale isochrones with a time-dependent helium abundance to Strömgren indices for 936 nearby F dwarfs. The dispersion about the mean relation at a fixed age is typically $\delta \approx 0.13$, most of which is accounted for by observational errors alone. A monotonic extrapolation to zero age gives $[\mathrm{Fe/H}]_1 \approx 0.06$, which agrees with other determinations to within the estimated uncertainties (reviewed by Mould 1982). We therefore adopt $Z_1 = 1.15\, Z_\odot \approx 0.022$ for the present metallicity in the solar neighbourhood and scale to this value when appropriate. From an extrapolation to low metallicities, we adopt $T_1 = 12\,\mathrm{Gy}$ for the age of the disc. Twarog has assigned larger ages to a few of the stars in his sample but the behaviour of the relation at this end is too poorly known for comparison with the models.

As a secondary guide to chemical enrichment, we use the metallicity distribution derived by Pagel & Patchett (1975) and shown in Fig. 2. This is based on the ultraviolet excesses of 133 G dwarfs in the RGO catalogue and is corrected for scale-heights. The metallicities are calibrated against the Hyades and, for conversion to $\log(Z/Z_1)$, we use $[\mathrm{Fe/H}]_{\mathrm{Hyades}} = 0.15$ (Crawford & Perry 1976). Previous investigators have compared the theoretical distribution $S(Z) \equiv \mu_s(Z)/\mu_s(Z_1)$ with a smoothed version of the data in integral form but we prefer to compare $dS(Z)/d\log Z$ with the data in differential form. The theoretical distribution is first convolved with a Gaussian in $\log Z$ to account for intrinsic and observational scatter in the metallicities at a fixed age; thus

$$\frac{dS(Z)}{d\log Z} \to \frac{1}{\sqrt{2\pi}\,\delta}\int_{-\infty}^{+\infty} d(\log Z')\,\frac{dS(Z')}{d\log Z'}\exp\left\{-[\log(Z/Z')]^2/2\delta^2\right\}. \qquad (15)$$

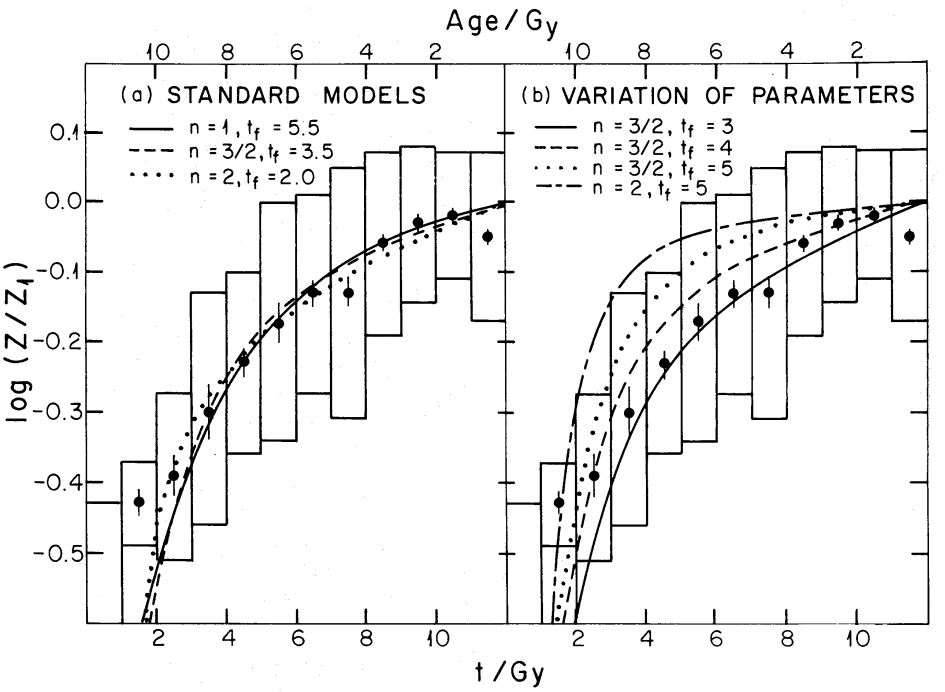

Figure 1. Metallicity as a function of age for F dwarfs in the solar neighbourhood. The data points are from Twarog (1980); the bars represent the standard error of the mean log Z in each age bin and the boxes represent the standard deviations of individual measurements from the mean. (a) Standard models of Table 1. (b) Variation of n and t_f for models with $q = 2$, $\beta = 17$, $\sigma_{s0} = 3$. The parameter C was adjusted to give $\mu_g(T_1) \approx 6$; thus $C = (1.0, 1.3, 1.7, 7.4)$ in the order that the models are listed in the legend above.

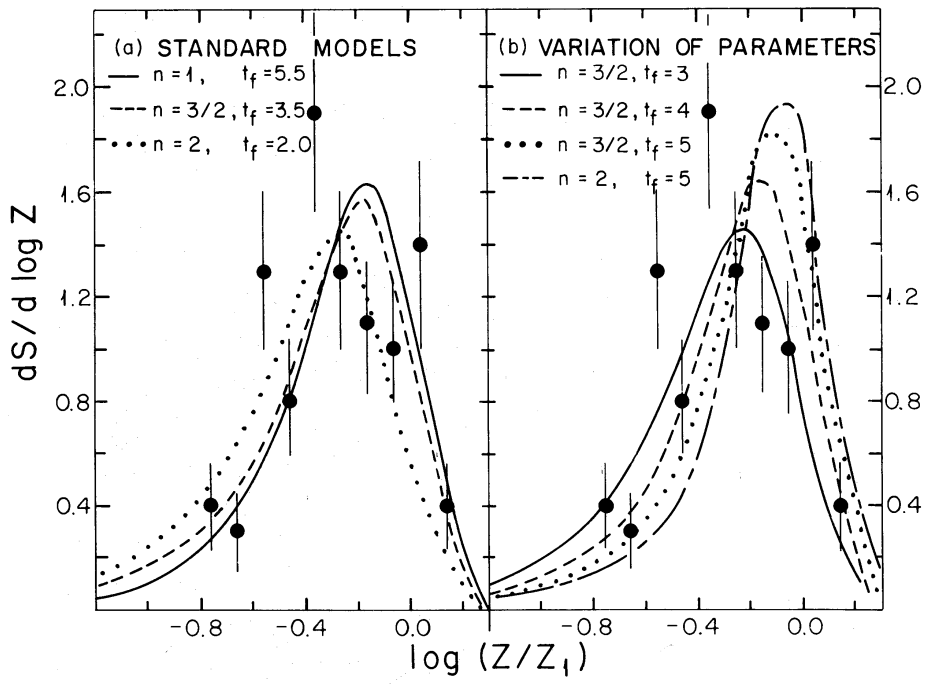

Figure 2. Normalized distribution of metallicities for G dwarfs in the solar neighbourhood. The data points are from fig. 6 of Pagel & Patchett (1975) and the bars represent $\sqrt{N}$ uncertainties in each metallicity bin. The models are the same as in Fig. 1(a) and (b).

For the dispersion, we adopt $\delta = 0.15$, which is consistent with the estimate of Pagel & Patchett.

3.2 STAR FORMATION AND INFALL RATES IN THE SOLAR NEIGHBOURHOOD

The history of star formation in our models is determined by fitting them to the distribution of metallicity and the relation between metallicity and age. In principle, $\psi(t)$ could be determined from a combination of the distribution of stellar ages with the initial mass function but in practice the method has large uncertainties. Nevertheless, Mayor & Martinet (1977) and Twarog (1980) have been able to place the useful limits, $1 \lesssim \bar{\psi}/\psi_1 \lesssim 3$, on the ratio of the past averaged to the present rate of star formation. An independent constraint on this ratio is provided the condition that the IMF be smooth near the present turnoff at $1 M_\odot$. From a detailed examination of this problem, Miller & Scalo (1979) infer $0.3 \lesssim \bar{\psi}/\psi_1 \lesssim 5$ with a constant IMF. They also claim that this excludes star formation rates with $n \gtrsim 0.5$ but their remarks are confined to models without infall.

An often quoted estimate of the present infall rate is $f_1 \approx 2 M_\odot\,\mathrm{pc}^{-2}\,\mathrm{Gy}^{-1}$ from Oort's (1970) analysis of the intermediate and high velocity clouds. This depends on the assumption that the clouds are accelerated toward the disc by the pressure of infalling gas and other interpretations now seem equally plausible (Bregman 1980 and references therein). An indirect constraint on infalling gas is that the radiation it emits while encountering the Galaxy should not exceed the soft X-ray background at high galactic latitudes. Cox & Smith (1976) derive the upper limit $1 M_\odot\,\mathrm{yr}^{-1}$ for the Galaxy as a whole, which corresponds to $f_1 \lesssim 1 M_\odot\,\mathrm{pc}^{-2}\,\mathrm{Gy}^{-1}$ in the solar neighbourhood. If there are no sources of deuterium other than primordial gas, then its present abundance in the interstellar medium can be used to put limits on the infall rate. In this way, Audouze *et al.* (1976) estimate $t_f \gtrsim 2\,\mathrm{Gy}$ for the Galactic Centre, which corresponds to $f_1 \gtrsim 0.1 M_\odot\,\mathrm{pc}^{-2}\,\mathrm{Gy}^{-1}$ in the context of our models.

3.3 KINEMATICAL EVOLUTION IN THE SOLAR NEIGHBOURHOOD

For the velocity dispersion of stars in the vertical direction, we use the two relations derived by Wielen (1974a) and shown in Figs 3 and 4. The first of these is based on the trigonometric parallaxes, proper motions, radial velocities and *UBV* colours of 159 dwarf stars in a kinematically unbiased subsample of Gliese's catalogue. The stars are weighted by the inverse of their crossing times through the plane in the computation of σ_s and are grouped by their main-sequence lifetimes τ_{ms}. To interpret the relation, Wielen (1977) assumes a constant star formation rate, which implies the mean age $\tau = \frac{1}{2}\tau_{ms}$ for each group, and finds $\sigma_s \propto \tau^{1/p}$ with $2 \lesssim p \lesssim 3$. This approach is not guaranteed to be consistent with our models and we therefore compare them directly with the relation between σ_s and τ_{ms}. The velocity dispersion of the stars born between $t = T_1 - \tau_{ms}$ and the present can be computed from equation (9) in a manner similar to that of equation (10). This gives

$$\sigma_s^2(\tau_{ms}) = \frac{q\{\sigma_{s0}^q + \beta[\mu_s(T_1) - \mu_s(T_1 - \tau_{ms})]\}^{2/q+1} - q\,\sigma_{s0}^{q+2}}{\beta(2+q)[\mu_s(T_1) - \mu_s(T_1 - \tau_{ms})]} \tag{16}$$

which depends explicitly on the star formation rate through $\mu_s(t)$.

The second relation derived by Wielen (1974a) is based on the trigonometric parallaxes, proper motions, radial velocities and calcium emission indices of 195 K and M dwarfs in a kinematically unbiased subsample of the McCormick catalogue. Ca II emission is known to correlate with relative age but the absolute ages $T_1 - t_L$ and $T_1 - t_U$ that bracket each HK class are uncertain. Wielen (1977) assumes a constant star formation rate and uses the known

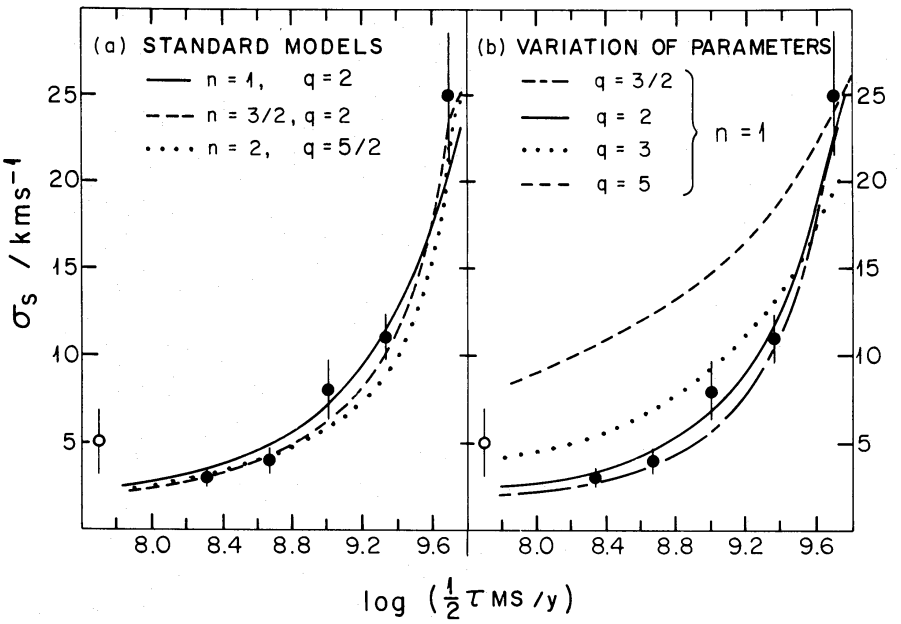

Figure 3. Velocity dispersion in the vertical direction as a function of main-sequence life-time for stars in the solar neighbourhood. The data points are from Wielen (1974a, b) and the bars represent standard errors. (a) Standard models of Table 1. (b) Variation of q for models with $n = 1$, $t_f = 5.5$, $C = 0.5$. β was adjusted to give $\sigma_{sm} \approx 25$ and σ_{s0} was adjusted to give agreement at small τ_{ms} when possible; thus $\beta = (3.0, 14, 250, 2.7 \times 10^5)$ and $\sigma_{s0} = (2, 2, 3, 4)$ in the order that the models are listed in the legend above.

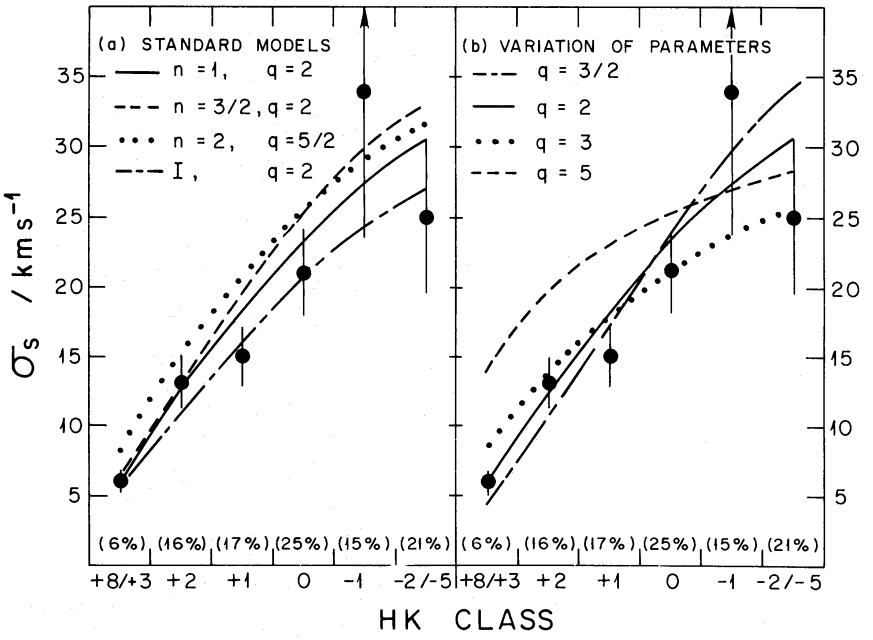

Figure 4. Velocity dispersion in the vertical direction as a function of HK class for K and M dwarfs in the solar neighbourhood. The data points are from Wielen (1974a) and the bars represent standard errors; the numbers in brackets give the fraction of stars in each HK class. The models are the same as in Fig. 3(a) and (b) with the addition of model I; this has $q = 2$, $\beta = 11$, $\sigma_{s0} = 3$ and is considered the best fit to these data alone.

fractions S_L and S_U of stars born in the unknown time intervals $0 < t \leqslant t_L$ and $0 < t \leqslant t_U$ to assign the mean age $\tau = T_1 - \frac{1}{2}(S_L + S_U)T_1$ to each class. This relation is also corrected for crossing times through the disc and leads to $2 \lesssim p \lesssim 3$. Again, we use equation (9) to generalize Wielen's approach to more realistic models; the result is

$$\sigma_s^2(\mathrm{HK}) = \frac{q[\sigma_{s0}^q + \beta(1-S_L)\mu_s(T_1)]^{2/q+1} - q[\sigma_{s0}^q + \beta(1-S_U)\mu_s(T_1)]^{2/q+1}}{\beta(2+q)(S_U - S_L)\mu_s(T_1)} \tag{17}$$

which depends implicitly on the star formation rate only through S_L and S_U.

3.4 PRESENT STRUCTURE OF THE STELLAR DISC

The assumption that the central surface brightness in the disc component of our Galaxy is typical of face-on galaxies and the estimated surface brightness in the solar neighbourhood imply $\alpha r_0 \approx 2.3$ for the galactocentric radius of the Sun in units of the exponential scale-radius (de Vaucouleurs & Pence 1978). With this in mind, we adopt $\alpha^{-1} = 4$ kpc and $r_0 = 9$ kpc and scale other quantities to these values when appropriate. For the total mass density in the solar neighbourhood, we adopt the estimate by Oort (1960) of $80\,M_\odot\,\mathrm{pc}^{-2}$, which is consistent with the Miller–Scalo (1979) IMF, a decreasing star formation rate and returned fractions in the range $0 \lesssim R \lesssim 0.5$. This implies $\mu_0 = 760\,M_\odot\,\mathrm{pc}^{-2}$ for the extrapolated central density of the disc if, as assumed here, its mass-to-light ratio is approximately constant. When condition (6) is used, the rotation velocity of the disc is taken to be $v_m = 220\,\mathrm{km\,s}^{-1}$.

The exponential scale-height of the stellar disc is determined by the local surface density and a representative velocity dispersion through equation (12). Since our models are fitted to Wielen's relations, which have $\sigma_{sm} \approx 25\,\mathrm{km\,s}^{-1}$ for all K and M dwarfs, they are guaranteed to give $h_s \approx 290$ pc in the solar neighbourhood. This is consistent with the direct estimate of $h_s = 300 \pm 50$ pc from counts of late-type stars at high galactic latitudes (Gilmore & Reid 1983 and references therein). From an analysis of all the open clusters with known distances and ages, Janes & Adler (1982) conclude that the galactic disc thickens with increasing galactocentric radius. However, most of the clusters in this sample are so young that their distribution is more representative of the gas from which they formed than it is of the stellar disc as a whole. The thickening persists for the 40 clusters older than 10^9 yr but this may in part be the result of a disruption rate that decreases with galactocentric radius.

A more reliable indication of the radial dependence of the scale-height is provided by van der Kruit & Searle's (1981a, b, 1982) photometry of seven edge-on galaxies. In all cases, the disc components can be fitted by the projection on the sky of a model with h_s constant and a radial cut-off at r_{max}. The sample mean and standard deviation for these parameters are $h_s = 420 \pm 160$ pc, which derives from a Hubble constant of $75\,\mathrm{km\,s}^{-1}\,\mathrm{Mpc}^{-1}$ and $\alpha r_{max} = 4.7 \pm 0.7$, which is independent of the distance scale. The maximum radial variation of h_s that would be compatible with van der Kruit & Searle's photometry is difficult to judge but it probably cannot be more than a factor of 2 over the range $1 \lesssim \alpha r \lesssim 4$. Equation (13) then implies that the diffusion exponent is bracketed by $1.6 \lesssim q \lesssim 2.6$, with higher values in the range corresponding to a scale-height that increases outward. The relatively narrow spread in h_s between galaxies is consistent with our assumption that the parameter β is a constant in the models.

3.5 PRESENT STRUCTURE OF THE GASEOUS DISC

For the distribution of neutral atomic hydrogen in the radial range $4\,\mathrm{kpc} \lesssim r \lesssim 14\,\mathrm{kpc}$, we rely on the analysis by Gordon & Burton (1976). Our estimates of the distribution of

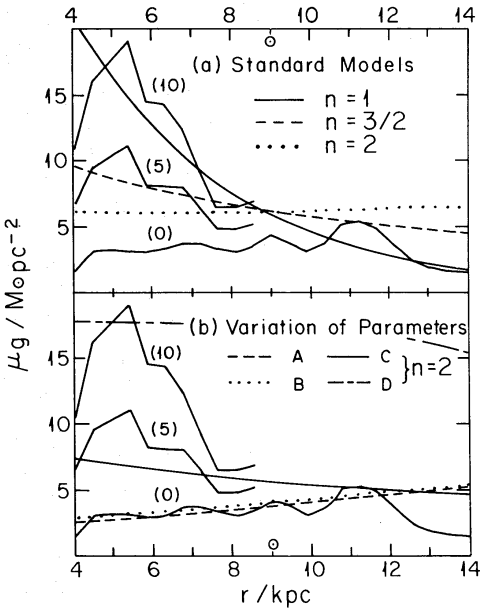

Figure 5. Gas density as a function of galactocentric radius. The empirical distributions have been computed from the H I data of Gordon & Burton (1976) and the CO data of Solomon & Sanders (1980) as described in Section 3.5; they are labelled by the corresponding values of $Q/10^5$. (a) Standard models of Table 1. (b) Variation of t_f and C for models with $n = 2$, $q = 2$, $\beta = 17$, $\sigma_{s0} = 3$; for A, $t_f = 0.1$, $C = 2.1$; for B, $t_f = 0.5$, $C = 2.1$; for C, $t_f = 5$, $C = 7.4$; for D, $t_f = 2$, $C = 0.35$.

molecular hydrogen are based on the emissivity data of Solomon & Sanders (1980) for carbon monoxide. The component of ^{13}CO is assumed to be optically thin and to be in local thermodynamic equilibrium with an excitation temperature of 12 K. For the parameter $Q \equiv n(H_2)/n(^{13}CO)$, we consider the range from $Q = 5 \times 10^5$, the value found by Dickman (1978) from the visual extinction in dark clouds, to $Q = 10 \times 10^5$, the value preferred by Liszt, Xiang & Burton (1981). The resulting surface densities of gas, which we assume to consist of H I plus H_2 and 25 per cent helium by mass, are shown in Fig. 5. They are slightly lower than the densities advocated by Solomon & Sanders (1980) and slightly higher than those advocated by Blitz & Shu (1980). The molecular component beyond the solar circle is uncertain but is probably smaller than the atomic component.

For the velocity dispersion of H I clouds in our Galaxy, Crovisier (1978) finds $6\,km\,s^{-1}$. Stark (1979) estimates a dispersion of $8\,km\,s^{-1}$ in the velocities of molecular clouds and Liszt *et al.* (1981) find that the scatter in the terminal velocities of CO emission can be represented by a dispersion of $4\,km\,s^{-1}$. High-resolution studies of several nearby galaxies show that the velocity dispersions in their H I layers are about $9\,km\,s^{-1}$ at all radii (reviewed by Baldwin 1981), which is consistent with our assumption that σ_g is a constant in the models. As a compromise between these values, we adopt $\sigma_g = 6\,km\,s^{-1}$ for the velocity dispersion of the gas in our Galaxy. The corresponding half-thickness, as approximated by equation (11), increases from $H_g \approx 60$ pc at $r = 4$ kpc to $H_g \approx 110$ pc in the solar neighbourhood and then to $H_g \approx 250$ pc at $r = 14$ kpc. When the adopted values of σ_g and v_m are inserted in condition (6) star formation is prevented beyond $r_{max} \approx 4.1\alpha^{-1} \approx 16$ kpc, even though the gas layer extends to larger radii.

3.6 RADIAL VARIATIONS IN METALLICITY AND STAR FORMATION RATE

As an indication of metallicity in the radial range $4\,kpc \lesssim r \lesssim 14\,kpc$, we use the two relations shown in Fig. 6. The first is based on DDO and *UBV* photometry of 41 open clusters

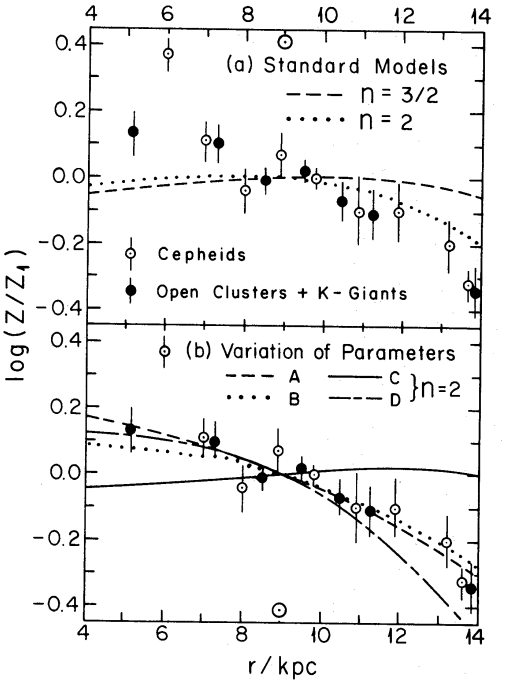

Figure 6. Stellar metallicity as a function of galactocentric radius. The data points for K giants and open clusters are from Janes (1979) and those for classical Cepheids are from Harris (1981) as presented by Mould (1982); the bars represent standard errors of the mean log Z in each radial bin. The models are the the same as in Fig. 5(a) and (b) with the ommission of the $n = 1$ standard model, which has $Z = Z_1$ at all radii.

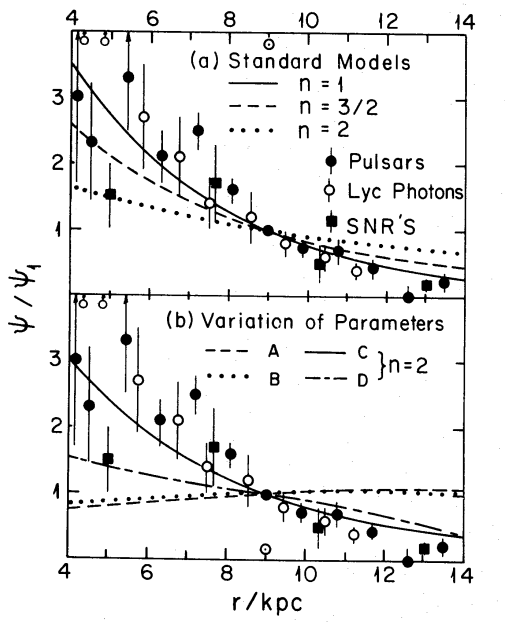

Figure 7. Radial distribution of star formation tracers. The data points for the pulsars and supernova remnants are from Lyne *et al.* (1983, in preparation) and Guibert *et al.* (1978) respectively; the bars represent $\sqrt{N}$ uncertainties in each radial bin of these distributions. The data points for the Lyman continuum photons are from Mezger (1978); in this case, the bars represent longitudinal fluctuations in the observed flux densities, which probably underestimate errors in the derived radial distribution. The models are the same as in Fig. 5(a) and (b).

and 79 K giants by Janes (1979) and the second is based on Washington photometry of 102 classical Cepheids by Harris (1981). Apart from the K giants, these objects are young enough that their metallicities should be representative of the interstellar medium in the recent past. To minimize any bias caused by an age spread or calibration errors, we have, however, scaled both relations to the same value of Z_1 in the solar neighbourhood. The average gradient, $d \log Z/dr = -(0.06 \pm 0.02)\,\mathrm{kpc}^{-1}$, is consistent with the oxygen abundances in the limited sample of galactic H II regions with measured electron temperatures (reviewed by Peimbert 1979). It is also typical of the oxygen gradients found in nearby galaxies after scaling to similar photometric radii (reviewed by Pagel & Edmunds 1981).

As tracers of star formation in the radial range $4\,\mathrm{kpc} \lesssim r \lesssim 14\,\mathrm{kpc}$, we use the three distributions of radio objects shown in Fig. 7. The first is based on the analysis by Lyne, Manchester & Taylor (1983, in preparation) of 316 pulsars in the Arecibo, Jodrell Bank, Molonglo and NRAO surveys and the second is based on the analysis by Guibert, Lequeux & Viallefond (1978) of 44 supernova remnants from the list of Clark & Caswell (1976). The third is the distribution of Lyc photons emitted by all O stars as derived by Mezger (1978) from the longitudinal variation of continuum radiation at 1.4 GHz. From a comparison of the radial and vertical distributions of several tracers of star formation with the gas in the galactic disc, Guibert *et al.* (1978) conclude that the Schmidt exponent probably lies in the range $1.3 \lesssim n \lesssim 2$. Madore (1977) has argued that the depletion of gas in regions of active star formation may lead to biased estimates of n but this does not affect the relation between ψ and μ_g on the scales of interest here.

4 Results of the models

4.1 STANDARD MODELS FOR THE SOLAR NEIGHBOURHOOD

We first computed a series of models for the solar neighbourhood over a large grid of input parameters. For each value of the star formation exponent, $n = 1$, 3/2, 2, we then chose as a 'standard' model the one that best represented the observational data of the previous section. The infall time-scale t_f and star formation coefficient C were fixed by the metallicity–age relation, the distribution of metallicities and the present gas density $\mu_g(T_1) \approx 6\,M_\odot\,\mathrm{pc}^{-2}$. The diffusion parameters q, β and σ_{s0} were fixed by the relation between velocity dispersion and main-sequence life-time and the relation between velocity dispersion and calcium emission. Our adopted values for these parameters are listed in Table 1 and their uncertainties are discussed in the next subsection. Several of the output relations are shown in the left-hand panels of Figs 1–4 and several of the output parameters are listed in Table 2.

All of the standard models have present infall rates that are compatible with the observational constraints mentioned in Section 3.2. The $n = 1$ and $n = 3/2$ models have values of $\bar{\psi}/\psi_1$ that lie within the range discussed in Section 3.2 but the $n = 2$ model has a value that lies above it. As Fig. 8 shows, this is caused by the peak in $\psi(t)$ at $t \approx 2$ Gy and the subsequent decline, which is more rapid for smaller values of t_f and therefore larger values of n. At the present epoch, gas is consumed by star formation 1.5 times faster than it is replenished by infall in the $n = 1$ model, 2 times faster in the $n = 3/2$ model and 7 times faster in the $n = 2$ model. The corresponding time-scales for gas depletion, $\mu_g(T_1)/[(1-R)\psi_1 - f_1]$, are 6, 8 and 10 Gy respectively. In units of $M_\odot\,\mathrm{pc}^{-2}\,\mathrm{Gy}^{-1}$, the present ejection rate of new metals, $y(1-R)\psi_1$, is 0.044 for $n = 1$, 0.022 for $n = 3/2$ and 0.008 for $n = 2$. The first of these agrees well with the theoretical estimates mentioned in Section 2.5, the second is probably acceptable but the third is almost certainly too low.

Table 1. Input parameters for the standard models.

n	t_f	C	q	β	σ_{so}
1	5.5	0.5	2	14	2
3/2	3.5	1.1	2	17	2
2	2.0	2.1	5/2	85	3

Units: t_f in Gy, C in $(M_\odot pc^{-3})^{1-n}$ Gy^{-1}, β in (km $s^{-1})^q$ $(M_\odot pc^{-2})^{-1}$, σ_{so} in km s^{-1}.

Table 2. Output parameters for the standard models.

n	y	$\bar{\psi}/\psi_1$	$(1-R)\psi_1$	f_1	σ_{sm}
1	0.015	2.1	2.9	1.9	23
3/2	0.014	3.9	1.6	0.8	25
2	0.012	8.6	0.7	0.1	25

Units: ψ_1 in $M_\odot pc^{-2}$ Gy^{-1}, f_1 in $M_\odot pc^{-2}$ Gy^{-1}, σ_{sm} in km s^{-1}.

4.2 VARIATION OF PARAMETERS FOR THE SOLAR NEIGHBOURHOOD

The effects of varying the input parameters that govern chemical enrichment are shown in the right-hand panels of Figs 1 and 2. For a given value of n, an increase in either t_f or C increases the curvature in the relation between $\log(Z/Z_1)$ and t/T_1 and shifts the peak in $dS(Z)/d\log Z$ to larger values of $\log(Z/Z_1)$. However, larger values of t_f raise $\mu_g(T_1)$ whereas larger values of C lower it. The present gas density is therefore the main discriminant between sets of infall time-scales and star formation coefficients that are compatible with the metallicity–age relation and the metallicity distribution. For 30 per cent uncertainties in $\mu_g(T_1)$, we estimate that t_f and C are uncertain by about 20 per cent when n is fixed. When n is adjusted upwards, t_f must be decreased to satisfy all of the available constraints.

The effects of varying the input parameters that govern stochastic acceleration are shown in the right-hand panels of Figs 3 and 4. For a given $\psi(t)$, an increase in q decreases the curvature in the relation between σ_s and $\log(\frac{1}{2}\tau_{ms})$ and increases the curvature in the relation between σ_s and HK class. Variations in β and σ_{s0} alter the young and old endpoints of these relations but have little effect on their curvature. The diffusion parameters influence the star formation rate only through the scale-height of the gas layer and the effects are always small. Conversely, n, t_f and C have no influence on σ_s(HK) and only a weak influence on $\sigma_s(\tau_{ms})$. Since the first relation is dominated by old stars and the second by young stars, q must be adjusted upwards if the peak in $\psi(t)$ is shifted to earlier times. Considering all the

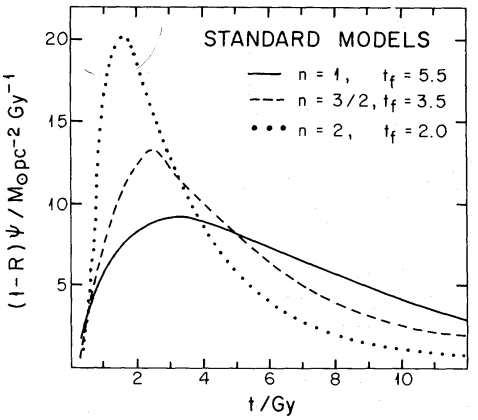

Figure 8. Star formation rate as a function of time for the standard models of Table 1.

uncertainties, we estimate $1.5 \lesssim q \lesssim 2.5$ as a reasonable range for the diffusion exponent and uncertainties of about 20 per cent in β and 40 per cent in σ_{s0} when q is fixed.

We have also investigated the effects of infall rates that differ from equation (3) on the chemical evolution of the solar neighbourhood. In one set of models, a fraction F_0 of the final mass accumulates suddenly at $t = 0$; thereafter, $F(t)$ decays exponentially with a time-scale t_f and is normalized to $1 - F_0$. For $F_0 \gtrsim 0.5$, more metal-poor stars are predicted than observed when t_f is adjusted to reproduce the metallicity–age relation. For $F_0 \lesssim 0.5$ both constraints can be satisfied although $F_0 \approx 0$ gives a somewhat better fit than other values in this range. In another set of models, $F(t)$ decays exponentially with a time-scale t_f for $0 < t \leqslant t_f$, is zero for $t_f < t \leqslant T_1$ and is normalized to unity. Again, too many metal-poor stars are predicted when t_f is adjusted to reproduce the metallicity–age relation. These results support our assumption that the infall rate decreases smoothly up to the present epoch.

4.3 MODELS WITH CONSTANT PARAMETERS FOR THE GALACTIC DISC

We next computed the evolution of the standard models over a large grid of galactocentric radii. The present metallicity, gas density and star formation rate are shown in the upper panels of Figs 5–7 for $4\,\text{kpc} \lesssim r \lesssim 14\,\text{kpc}$. This range was chosen because, outside 14 kpc, the density of stars is low and the data are sparse or non-existent. Inside 4 kpc, the gas probably has a significant component of radial motion and may have been depleted by winds from the bulge or sweeping by a bar. Between these limits, the $n = 1$ and $n = 3/2$ models produce gradients in $\mu_g(r)$ and $\psi(r)$ that are reasonably consistent with the empirical relations when allowance is made for the large uncertainties. However, the $n = 2$ model produces gradients in $\mu_g(r)$ and $\psi(r)$ that are weaker than permitted by the data and all three models fail to produce the observed gradient in $Z(r)$. Since μ_g/μ_s increases outward in the disc, this cannot be due to a breakdown in the approximation of instantaneous recycling.

In an attempt to improve the comparison with the observations, we computed another series of models with different values of t_f and C. Some of the results are shown in the lower panels of Figs 5–7 for $n = 2$, which always gave the largest metallicity gradient. For a given value of C, smaller values of t_f increases $|dZ/dr|$ and, in the extreme case that the models are essentially closed, the radial variation of metallicity can be brought into agreement with the empirical relation. However, smaller values of t_f always decrease $|d\mu_g/dr|$ and $|d\psi/dr|$ and therefore worsen the discrepancy with these relations. Changing C has an effect on dZ/dr, $d\mu_g/dr$ and $d\psi/dr$ that is qualitatively similar to changing t_f but with the opposite sign. Thus, no combination of these parameters will simultaneously reproduce the radial variations in metallicity, gas density and star formation rate, even when they are allowed to vary far from their values in the standard models.

We also computed a series of models that incorporate the instability condition (6). Since this delays the onset of star formation at each galactocentric radius until a time $t_*(r)$ that increases with r, it should help to produce a metallicity gradient. For the solar neighbourhood, the critical surface density is $23\,M_\odot\,\text{pc}^{-2}$ and the critical times are $t_* = 1.5$ Gy with $t_f = 5$ Gy and $t_* = 0.7$ Gy with $t_f = 2$ Gy. Our results show that the instability condition has a negligible effect on the chemical evolution at this radius and the standard models are not affected for $t \gtrsim t_*$. Similarly, the delay has little influence over most of the galactic disc although it does produce the expected cut-off at $r_{max} \approx 16$ kpc and a steep gradient in $Z(r)$ in a transition zone between 14 and 16 kpc.

4.4 MODELS WITH VARIABLE PARAMETERS FOR THE GALACTIC DISC

In another attempt to reproduce the observed gradients, we computed a series of models in which the infall time-scale and star formation coefficient vary with galactocentric radius. If

the disc is built up from material that was originally associated with the bulge or halo of the galaxy, t_f might be expected to increase outwards. The exact dependence is difficult to predict but it is not likely to be stronger than that of the free-fall time-scale, which varies as r/v_m and therefore by a factor of 3.5 between 4 and 14 kpc. If star formation is triggered by the passage of gas through a spiral density wave with a pattern frequency Ω_p, a relation of the form $C \propto |\Omega_p - v_m/r|$ might be expected to apply. The corotation radius of the galactic disc is usually assumed to be about 16 kpc, which suggests that C could decrease outwards by an order of magnitude or more between 4 and 14 kpc. Any reasonable dependence of t_f and C on radius ought to have values in the solar neighbourhood near those of the standard models.

For each radius we can determine what regions of the (t_f, C) plane give values of Z/y, μ_g and $(1-R)\psi$ that taken separately are compatible with the observations. If all three of the allowed regions overlap, the corresponding models are acceptable at that radius and if the regions overlap at all radii the dependence of C and t_f on radius is determined. The acceptable range for each quantity is based on our subjective assessment of the observational errors, which include the uncertainties in the conversion from $n(^{13}CO)$ to $n(H_2)$. (To convert from the observational quantities Z/Z_1 and ψ/ψ_1 to the theoretical quantities Z/y and $(1-R)\psi$ we use the values of Z_1/y and $(1-R)\psi_1$ given by the standard model for the solar neighbourhood with that value of n.) As Fig. 9 shows, marginal consistency is possible at $r = 5$ kpc, but there are no consistent solutions for $r = 14$ kpc. Since these are the most general models with fixed n, we conclude that some additional ingredient is needed to account for all the observed properties of the galactic disc.

4.5 EFFECTS NOT INCLUDED IN THE MODELS

The simplest way to reproduce the metallicity gradient in the galactic disc is to decrease the yield in the models by a factor of about 3 between radii of 4 and 14 kpc. Since there is no compelling evidence for the corresponding variations in the initial mass function, this solution seems rather arbitrary. Another possibility is to assume that the infalling gas is ejected from evolved stars in the galactic halo with a metallicity Z_f that decreases outward from the centre. Since Z_f should be roughly constant in time for $t \gtrsim 10^8$ yr, our previous results can be adapted to this case by the substitution $Z_g \to Z_g + Z_f$. If the metallicities of globular clusters are representative of those in the halo, the appropriate values might be $Z_f \sim 0.1\, Z_\odot$ in the inner parts and $Z_f \sim 0.01\, Z_\odot$ in the outer parts. The exact values depend on the adopted calibration of the metallicity-scale and the gradient could be weaker (Zinn 1980). In any case, the effects of this kind of infall on our previous results appear to be negligible.

A more promising explanation of the metallicity gradient in the galactic disc is in terms of radial gas flows. These might be driven by the infall of gas with less rotation than that required for circular motion at the point of impact on the disc, which would promote an inward drift. Alternatively, such flows might be driven by a bar or spiral density wave although the sign of this effect is not known. A flow with a net radial velocity v_r would produce a metallicity gradient of order $y\psi/v_r\mu_g$ after a time of order $r/|v_r|$ (Tinsley 1980). Thus, if v_r were a few km s^{-1} inwards, the observed gradient could be built up over the lifetime of the disc. The existing observations of HI in the galactic centre and anti-centre directions appear to be consistent with no radial motion of the gas but the uncertainties are probably large enough to allow $|v_r| \lesssim 5$ km s^{-1} (Weaver & Williams 1974). A flow with this velocity would have a negligible effect on the stochastic acceleration of the stars and would not alter our conclusions about the radial dependence of their scale-height.

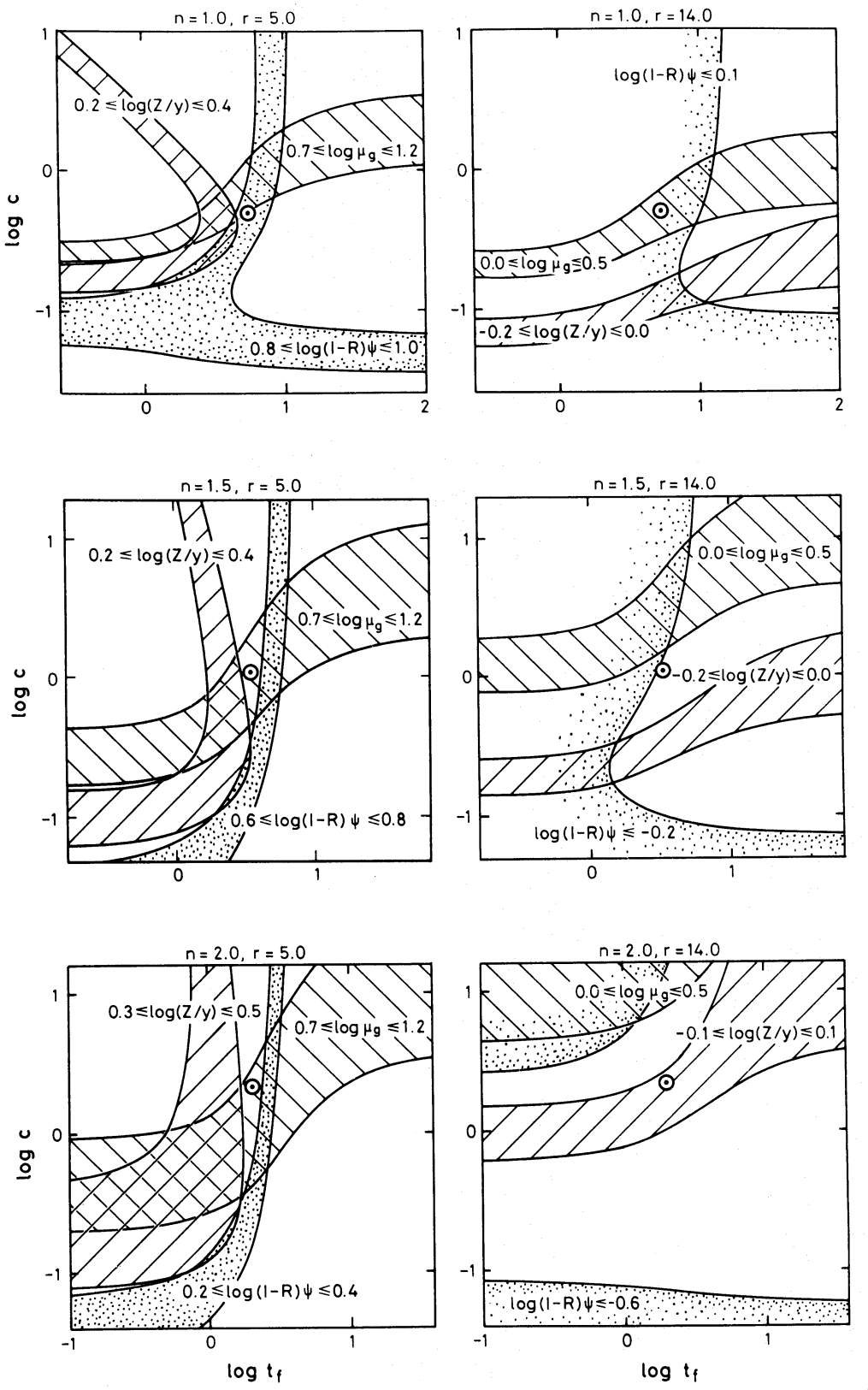

Figure 9. Observational constraints on the radial dependence of the infall time-scale and star formation coefficient. The shaded regions show the models with $n = 1$, $3/2$ and 2 that are compatible with the data at $r = 5$ kpc and $r = 14$ kpc. The open circles show the values of t_f and C in the standard models with the corresponding value of n. The ranges of values indicated for μ_g, Z/y and $(1-R)\psi$ are based on the observations shown in Figs 5, 6 and 7 and on our subjective assessment of their uncertainties.

To estimate the kinematical effects of infall, we assume that the motions of stars are approximately harmonic in the vertical direction. In this case, the adiabatic invariant is ϵ/ω where ϵ is the orbital energy and $\omega \propto (\mu_{\rm tot}/H_{\rm s})^{1/2}$ is the orbital frequency. Averaging over the stellar distribution gives $\langle \epsilon \rangle \propto \sigma_{\rm s}^2$ so that $\sigma_{\rm s}^3/\mu_{\rm tot}$ is approximately constant. If there were no other sources of acceleration, the velocity dispersion at time t of stars born at time t_0 would be

$$\sigma_{\rm s}(t;\, t_0) = \sigma_{\rm s0} \left[\frac{1-\exp(-t/t_{\rm f})}{1-\exp(-t_0/t_{\rm f})} \right]^{1/3} \tag{18}$$

with our adopted infall rate. This implies $\sigma_{\rm s}(T_1;\, t_0) \lesssim 1.2\,\sigma_{\rm s0}$ for $t_0 \gtrsim t_{\rm f}$ and $\sigma_{\rm s}(T_1;\, t_0) \lesssim 2.2\,\sigma_{\rm s0}$ for $t_0 \gtrsim 0.1\,t_{\rm f}$, the latter covering the time interval over which the adiabatic approximation is valid in our models. Thus, the velocity dispersions predicted by this mechanism are only a few km s^{-1} and their dependence on the stellar ages, $\tau = T_1 - t_0$, differs markedly from the relations shown in Figs 3 and 4.

4.6 COMPARISONS WITH PREVIOUS WORK

Our models for the solar neighbourhood are most directly comparable with those of Vader & de Jong (1981). They treat infall and star formation in essentially the same way and find similar results for the chemical evolution after integration through the disc. Their diffusion coefficient for the stochastic acceleration of stars is proportional to the gas density rather than the star formation rate but the two treatments are nearly equivalent when the Schmidt exponent is $n = 1$. In this case, their index m is related to our index q by $m \approx q - 1$ because they include an extra factor of $H_{\rm g}/H_{\rm s} \approx \sigma_{\rm g}/\sigma_{\rm s}$ in their analogue of our equation (8). In contrast to our conclusions, Vader & de Jong prefer models with $q \approx 6$. This is based on a comparison with the observations that gives most weight to the present distribution of vertical velocities and least weight to the relations between velocity dispersion and age. Their results are therefore sensitive to uncertainties in the history of star formation and assumptions about the stellar distribution function whereas our results are not sensitive to these effects.

Our models for the radial properties of the galactic disc can only be compared in a rough way with previous work. Chiosi (1980) has presented several models that include the infall of metal-free gas and a star formation rate governed by Schmidt's prescription with $n = 2$. Our results for this case are similar to his although he claims that the models produce metallicity gradients in agreement with the observations. The models by Tosi (1982) produce metallicity gradients by specifying the infall and star formation rates as pre-determined functions of radius and time. This approach simply side-steps all questions concerning causal effects in the evolution of the disc. Mayor & Vigroux (1981) have presented an illustrative model with radial gas flows that are assumed to be driven by the infall of non-rotating and metal-free gas. This model reproduces the observed metallicity gradient but whether it also satisfies the constraints on chemical evolution in the solar neighbourhood is not yet clear.

5 Conclusions

In our models, the effects of infall, star formation, stochastic acceleration and chemical enrichment are governed by a small set of reasonable but idealized equations. This formulation is intended to strike a balance between physical assumptions that are too specific for

theoretical justification and those that are too general for observational verification. As a result, our models have fewer input parameters and the output relations are compared with a greater variety of observational material than is customary in this field. Some of the most useful constraints involve a combination of data from the solar neighbourhood with data from other parts of the galactic disc or nearby galaxies. This leads to a reasonably consistent picture of stochastic acceleration and emphasizes the need for a more complete picture of chemical enrichment. We plan to return to these points in subsequent investigations.

In summary, our main conclusions are the following. (1) Models with star formation exponents and infall time-scales $n = 1$ and $t_f = 5.5$ Gy or $n = 3/2$ and $t_f = 3.5$ Gy satisfy all the constraints on chemical evolution in the solar neighbourhood. The star formation rate probably declines too rapidly and the present ejection rate of new metals is probably too low in models with $n = 2$ to be consistent with observations. (2) The relation between the velocity dispersions in the vertical direction and the ages of stars in the solar neighbourhood requires that the exponent for stochastic acceleration lies in the range $1.5 \lesssim q \lesssim 2.5$. This brackets the values needed to explain the nearly constant scale-heights observed in the stellar discs of edge-on galaxies. (3). The models that are successful in the solar neighbourhood also reproduce the observed variation of gas density and star formation rate between galactocentric radii of 4 and 14 kpc but they do not reproduce the observed gradient in metallicity. The most promising cure for this discrepancy appears to be radial gas flows within the disc.

Acknowledgments

We thank our colleagues in Cambridge and Princeton, particularly Dr J. E. Gunn, for helpful discussions. We are also grateful to Dr J. H. Taylor for making available unpublished data on the radial distribution of pulsars. CGL acknowledges receipt of an SRC studentship and SMF acknowledges partial support from NSF grant PHY79-19884 to the Institute for Advanced Study.

References

Arnett, W. D., 1978. *Astrophys. J.*, **219**, 1008.
Audouze, J., Lequeux, J., Reeves, H. & Vigroux, L., 1976. *Astrophys. J.*, **208**, L51.
Baldwin, J. E., 1981. In *The Structure and Evolution of Normal Galaxies*, p. 137, eds Fall, S. M. & Lynden-Bell, D., Cambridge University Press.
Barbanis, B. & Woltjer, L., 1967. *Astrophys. J.*, **150**, 461.
Blaauw, A., 1965. In *Galactic Structure: Stars and Stellar Systems*, Vol. V, p. 435, eds Blaauw, A. & Schmidt, M., Chicago University Press.
Blitz, L. & Shu, F. H., 1980. *Astrophys. J.*, **238**, 148.
Bregman, J. N., 1980. *Astrophys. J.*, **236**, 577.
Chiosi, C., 1980. *Astr. Astrophys.*, **83**, 206.
Clark, D. H. & Caswell, J. L., 1976. *Mon. Not. R. astr. Soc.*, **174**, 267.
Cox, D. P. & Smith, B. W., 1976. *Astrophys. J.*, **203**, 361.
Crawford, D. L. & Perry, C. L., 1976. *Publ. Astr. Soc. Pacific*, **88**, 454.
Crovisier, J., 1978. *Astr. Astrophys.*, **70**, 43.
de Vaucouleurs, G. & Pence, W. D., 1978. *Astr. J.*, **83**, 1163.
Dickman, R. L., 1978. *Astrophys. J. Suppl.*, **37**, 407.
Fall, S. M. & Efstathiou, G., 1980. *Mon. Not. R. astr. Soc.*, **193**, 189.
Fujimoto, M., 1980. *Publ. astr. Soc. Japan*, **32**, 89.
Gilmore, G. & Reid, N., 1983. *Mon. Not. R. astr. Soc.*, **202**, 1025.
Goldreich, P. & Lynden-Bell, D., 1965. *Mon. Not. R. astr. Soc.*, **130**, 125.
Gordon, M. A. & Burton, W. B., 1976. *Astrophys. J.*, **208**, 346.
Guibert, J., Lequeux, J. & Viallefond, F., 1978. *Astr. Astrophys.*, **68**, 1.
Harris, H. C., 1981. *Astr. J.*, **86**, 707.

Janes, K. A., 1979. *Astrophys. J. Suppl.*, **39**, 135.
Janes, K. & Adler, D., 1982. *Astrophys. J. Suppl.*, **49**, 425.
Julian, W. H., 1967. *Astrophys. J.*, **148**, 175.
Larson, R. B., 1972. *Nature Phys. Sci.*, **236**, 7.
Larson, R. B., 1976. *Mon. Not. R. astr. Soc.*, **176**, 31.
Larson, R. B., 1977. In *The Evolution of Galaxies and Stellar Populations*, p. 97, eds Tinsley, B. M. & Larson, R. B., Yale University Observatory, New Haven.
Liszt, H. S., Xiang, D. & Burton, W. B., 1981. *Astrophys. J.*, **249**, 532.
Madore, B. F., 1977. *Mon. Not. R. astr. Soc.*, **178**, 1.
Maeder, A., 1981. *Astr. Astrophys.*, **101**, 385.
Mayor, M. & Martinet, L., 1977. *Astr. Astrophys.*, **55**, 221.
Mayor, M. & Vigroux, L., 1981. *Astr. Astrophys.*, **98**, 1.
Mezger, P. G., 1978. *Astr. Astrophys.*, **70**, 565.
Miller, G. E. & Scalo, J. M., 1979. *Astrophys. J. Suppl.*, **41**, 513.
Mould, J. R., 1982. *A. Rev. Astr. Astrophys.*, **20**, 91.
Oort, J. H., 1960. *Bull. astr. Inst. Netherlands*, **15**, 42.
Oort, J. H., 1970. *Astr. Astrophys.*, **7**, 381.
Pagel, B. E. J., 1981. In *The Structure and Evolution of Normal Galaxies*, p. 211, eds Fall, S. M. & Lynden-Bell, D., Cambridge University Press.
Pagel, B. E. J. & Edmunds, M. G., 1981. *A. Rev. Astr. Astrophys.*, **19**, 77.
Pagel, B. E. J. & Patchett, B. E., 1975. *Mon. Not. R. astr. Soc.*, **172**, 13.
Peimbert, M., 1979. In *The Large-Scale Characteristics of the Galaxy*, p. 307, ed. Burton, W. B., Reidel, Dordrecht, Holland.
Schmidt, M., 1959. *Astrophys. J.*, **129**, 243.
Schmidt, M., 1963. *Astrophys. J.*, **137**, 758.
Solomon, P. M. & Sanders, D. B., 1980. In *Giant Molecular Clouds in the Galaxy*, p. 41, eds Solomon, P. M. & Edmunds, M. G., Pergamon, Oxford.
Spitzer, L. & Schwarzschild, M., 1951. *Astrophys. J.*, **114**, 385.
Spitzer, L. & Schwarzschild, M., 1953. *Astrophys. J.*, **118**, 106.
Stark, A. A., 1979. *PhD thesis*, Princeton University.
Talbot, R. J. & Arnett, W. D., 1971. *Astrophys. J.*, **170**, 409.
Talbot, R. J. & Arnett, W. D., 1975. *Astrophys. J.*, **197**, 551.
Tinsley, B. M., 1980. *Fundamentals of Cosmic Physics*, **5**, 287.
Tinsley, B. M., 1981. *Astrophys. J.*, **250**, 758.
Tosi, M., 1982. *Astrophys. J.*, **254**, 699.
Twarog, B. A., 1980. *Astrophys. J.*, **242**, 242.
Vader, J. P. & de Jong, T., 1981. *Astr. Astrophys.*, **100**, 124.
van den Bergh, S., 1962. *Astr. J.*, **67**, 486.
van der Kruit, P. C. & Searle, L., 1981a. *Astr. Astrophys.*, **95**, 105.
van der Kruit, P. C. & Searle, L., 1981b. *Astr. Astrophys.*, **95**, 116.
van der Kruit, P. C. & Searle, L., 1982. *Astr. Astrophys.*, **110**, 61.
Weaver, H. & Williams, D. R. W., 1974. *Astr. Astrophys. Suppl.*, **17**, 1.
Wielen, R., 1974a. *Highlights Astr.*, **3**, 395.
Wielen, R., 1974b. *Astr. Astrophys. Suppl.*, **15**, 1.
Wielen, R., 1977. *Astr. Astrophys.*, **60**, 263.
Zinn, R., 1980. *Astrophys. J.*, **241**, 602.